Article

Principal Component Analysis of Blast Furnace Drainage Patterns

Mauricio Roche *, Mikko Helle and Henrik Saxén

Thermal and Flow Engineering Lab, Åbo Akademi University, 20500 Turku, Finland

* Correspondence: mroche@abo.fi

check for
updates

Abstract: Monitoring and control of the blast furnace hearth is critical to achieve the required production levels and adequate process operation, as well as to extend the campaign length. Because of the complexity of the draining, the outflows of iron and slag may progress in different ways during tapping in large blast furnaces. To categorize the hearth draining behavior, principal component analysis (PCA) was applied to two extensive sets of process data from an operating blast furnace with three tapholes in order to develop an interpretation of the outflow patterns. Representing the complex outflow patterns in low dimensions made it possible to study and illustrate the time evolution of the drainage, as well as to detect similarities and differences in the performance of the tapholes. The model was used to explain the observations of other variables and factors that are known to be affected by, or affect, the state of the hearth, such as stoppages, liquid levels, and tap duration.

Keywords: hearth; drainage; PCA; analysis tool; pattern; tapholes

---

1. Introduction

The blast furnace represents the most relevant process on the main route for ore-based production of iron in the steelmaking industry. An important part of the process is its lowest region, better known as the hearth, where molten iron and slag are collected before they are drained ("tapped") out through the tapholes. In large-size furnaces, this drainage procedure is carried out by opening alternating tapholes from where both liquid phases are tapped out simultaneously. Different tapping rates may occur, partly because of differences in the production or internal conditions in the hearth, leading to variation of the levels of the liquid phases. The outflow rates are anticipated to be lower in the beginning of the tapping, increasing as the drainage proceeds owing to erosion of the taphole. The erosion may be further induced by the arrival of newly produced hotter liquids that have not experienced heat loss to the hearth lining. The goal is to drain sufficient amounts according to observations and estimations to keep the liquid levels low in the furnace [1,2].

In large-scale operation, productivity and efficient operation of the casthouse might be jeopardized by the variation of operating factors. Some of the most common concerns are liquid-level fluctuations caused by production/extraction imbalance, and erosion of the hearth lining. Because of the complexity of the process and besides the lack of direct measurements, the understanding and control of the tapping procedure represent both difficult and essential tasks in order to ensure an efficient operation.

Earlier studies of alternating tapping practice presented differences in taphole length, amounts of liquids extracted, and hot metal temperature between the operating tapholes [1,3,4]. Even though some correlations among production variables and erosion of both lining and taphole were established, little is known about what induces such variations and how. Computational fluid dynamics (CFD) simulations were undertaken with the goal to clarify the relation between production variables, implicitly or explicitly suggesting that there may be considerable spatial distribution of the variables or differences depending on local conditions at the tapholes [5–8].

Many previous efforts have been made to shed light on the hearth fluid dynamics and the phenomena that occur during and between the taps. In contrast to earlier notions, the fact that iron can be drained to levels below the taphole was clarified in the 1980s by Tanzil et al. [9], who made small-scale experiments supported by computational analysis. The investigators showed that the flow of the viscous slag phase leads to a lower pressure in front of the taphole, which makes it possible to elevate iron from levels well below the taphole, thus leading to simultaneous outflow of the two liquid phases. Nouchi et al. [3] presented experimental work that associated slag ratio (mass ratio of slag to iron) with liquid levels and tap duration, as well as how the time corresponding to a maximum of the slag ratio shifted with changes in the conditions. Furthermore, the results showed that at constant conditions, the maximum slag ratio increases if low-permeability zones are present in the hearth. On the other hand, Nishioka et al. [10] pointed out that only taphole mud quality or erosion of the operating taphole could not explain the duration of the tapping and the fluctuations in the drainage rate. Even though some causal factors have been identified or suggested, little is reported about the occurrence or frequency of such fluctuations. Iida et al. [2] reached similar conclusions to Nishioka et al. [10], also suggesting that coke particle size and configuration in front of the taphole play important roles for the liquid outflow rates. These results indicate that local conditions at the taphole might cause such imbalance. Furthermore, in later efforts [1], the authors developed a mathematical model that led them to conclude that discrepancies between operating tapholes in terms of liquid drainage rate and tap duration were the result of local zones of low permeability. According to their model, the metal fraction depended on the vertical level of the iron–slag interface compared with the taphole level.

Several studies in the literature have presented models of hearth drainage [1,2,10–13]. A recent study by the present authors proposed a simple offline model simulating the liquid level fluctuations in a hearth with intermittent tapping [14]. By applying different conditions to each taphole, it was demonstrated that some outflow patterns and slag delays observed in a blast furnace could be mimicked. Thus, the model makes it possible to theoretically evaluate the role of different parameters. Furthermore, an online liquid-level model was also proposed based on similar simplifications and assumptions, but using estimates of the production and outflow rates [4]. The model considers a division of the hearth into pools with individual liquid levels. Its application indicated non-uniform drainage among the tapholes, as well as periods of accumulation and depletion of both iron and slag. However, certain drainage behaviors were observed that could not be explained by the models, so a deeper understanding of the hearth drainage behavior is needed. An analysis of the recurrence of outflow patterns and transition from one to another could provide some understanding of the blast furnace hearth state, even though irregularities frequently seen in the data make it difficult to identify and categorize the observations in an appropriate way. It is thus clear that a data-driven analysis of the liquids outflow patterns could be useful. The present paper addresses this very problem using principal component analysis to compress the information to make it easier to understand and illustrate.

2. Principal Component Analysis

The main purpose of principal component analysis (PCA) is to reduce the dimensionality of multivariate data. The method also provides guidelines on the number of components needed to represent the data in question with sufficient accuracy.

Consider a sample data Y of mean-centered measurements with n observations on q variables [15,16]. First, the linear combination $t_1 = Yp_1$ is found that accounts for the maximum variance subject to $|p_1| = 1$. This represents the first principal component. The second component is a combination defined by $t_2 = Yp_2$ that has the next greatest variance subject to $|p_2| = 1$ with the conditions that it is uncorrelated with, and orthogonal to, the first component t_1. The following components are similarly determined. The sample principal component loading vectors p_i are the eigenvectors of the covariance matrix of Y. PCA decomposes the observation matrix Y as

$$Y = TP^T = \sum_{i=1}^{q} t_i P_i^T. \tag{1}$$

If a considerable part of the variation is represented by the contribution of a smaller number of components, these components can replace the original data.

The present paper aims to identify and classify iron and slag outflow patterns from a reference blast furnace by applying PCA to two data sets. The data representation in lower-dimensional components is presented in the following section in order to identify and visualize possible trends in the drainage patterns. Some interpretations of the results will also be presented with respect to hearth dynamics and tapping procedure.

3. Method and Data Sets

The data analyzed consists of two data sets, Data set 1 and 2, of three and six months worth of measurements of liquid outflow rates, respectively, from a large blast furnace with three tapholes, TH-1, TH-2, and TH-3. Between the end of Data set 1 and the beginning of Data set 2, 15 months of operation passed. The iron outflow rate was obtained from torpedo weighing, while the slag outflow rate was estimated based on measurements from the granulation unit. Both signals were available as one-minute averages. Considering the recorded times from the individual taps, the liquid outflow rate for each tapping was calculated, resulting in a total of 887 consecutive ones for Data set 1 and 1729 for Data set 2. From here on, individual tapping samples will be referred as taps, while tapping will refer to the drainage process.

3.1. Pre-Processing of the Data Set

After visual inspection of the samples, systematic abrupt changes of the iron outflow rate (>5 tonne/min in a couple of minutes) were noticed, which did not agree with the overall trend. Such deviations were found to be caused by torpedo changes, so they were filtered out of the samples. The outflow samples were subjected to additional pre-processing conditions in order to discard samples that, owing to error in the measurements or records, could potentially corrupt the classification. Among these conditions were the following:

- outflow near zero for any of the phases;
- taps shorter than 40 min that may occur as a result of disturbances, stoppages, or contingencies;
- any of the phases shows an outflow rate above 2% of the production rate at all times (i.e., also during the intercast period, where there should be no liquid outflows); and
- the total outflow abruptly goes near zero as a result of measurement errors or possibly taphole clogging.

After excluding such samples, 776 taps remained in Data set 1 and 1463 taps in Data set 2, accounting for 87% and 86% of the original data sets, respectively. Nonetheless, the excluded samples were taken into account when estimating the slag delay (see below).

It was found to be appropriate to use a threshold for the outflow rate, set at 2% of the production rate, to indicate when the flow of the liquid in question (iron or slag) has started during the tap. This condition was needed as liquids from a tap often progressed in the runner to the torpedo and the granulation units for some minutes after the tapping ended, and so, based on this information, the moments when iron and slag started flowing out were noted, and the difference between these two times is called "slag delay" in what follows. Note that a negative slag delay means that slag starts flowing out first. The slag delay has an important meaning as it reflects the vertical location of the iron–slag interface in the hearth at the moment when the taphole is opened; therefore, it is an important feature to identify with the present method. Figure 1 illustrates two cases where different locations of the iron–slag interface determine which liquid phase will be "seen" first, that is, if the slag delay will

be positive or negative. The figure depicts the state of the interfaces just before the tapping ends (solid lines), just after the tap has ended and the interfaces have become horizontal (dotted lines) and the state just before the next tapping starts (dashed lines). In case (a), the right taphole has drained more slag and less iron, so the iron–slag interface is not significantly below the left taphole as the tapping ends, and while the tapholes are plugged, it rises above the left taphole. This will result in a positive slag delay in the following tap from the left taphole. As this taphole will start with iron-only flow, slag keeps on accumulating in the hearth, elevating the slag–gas interface. The duration of the tap is long and the iron–slag interface will have time to descend well below the taphole, eventually leading to the state depicted in the right panel, yielding a negative slag delay for the right taphole, as shown in case (b).
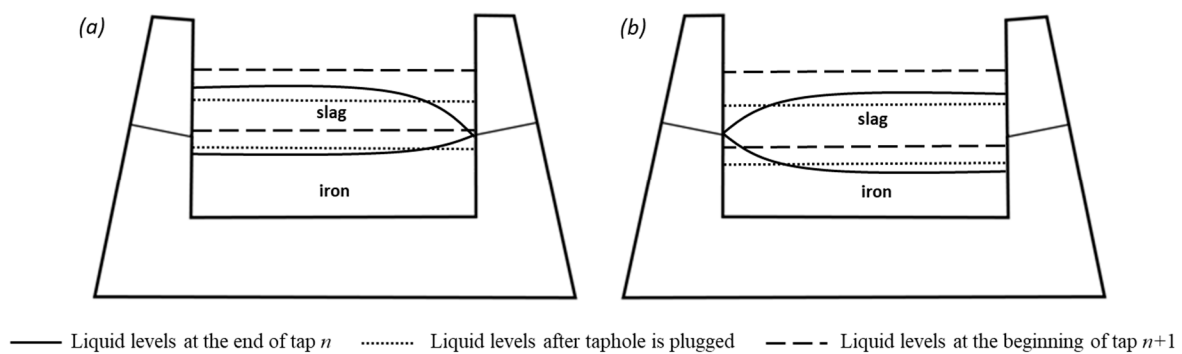

Figure 1. Illustration of two cases of slag delay: (**a**) positive slag delay (for the left taphole), (**b**) negative slag delay (for the right taphole).

PCA is a scale-dependent method. Thus, if the data matrix has variables of considerably bigger magnitude than others, these will have dominant weights in the sub-dimension. Therefore, the outflows were normalized by calculating the slag share, defined as

$$S_{\text{slag}}(i) = \frac{m_{\text{slag}}(i)}{m_{\text{iron}}(i) + m_{\text{slag}}(i)}, \tag{2}$$

where i denotes the time, while $m_{\text{iron}}(i)$ and $m_{\text{slag}}(i)$ are the corresponding mass flow rates of iron and slag from the furnace for the same time. The share of slag was considered an interesting variable, because work by other investigators has demonstrated that the hearth state may affect the distribution of the two liquids in the taps from multi-taphole furnaces [2,3,10]. Furthermore, in order to normalize the tap duration (defined as the time elapsed between the moment when the first liquid starts flowing out till the last liquid stops flowing out of the taphole), S_{slag} was down-sampled to 10 average points, each representing one tenth of the duration of the tap. Thus, all taps were represented by ten values of the slag share, which facilitated a comparison between the results of different taps despite differences in tap duration. This down-sampling was found to yield an acceptable representation of the variable without losing much significant or relevant information. Thus, the vector length of the samples to be categorized was of 10. The method aims to identify outflow patterns within the production levels of the BF; therefore, both slag fraction and tapping duration were required to results pattern-dependent. Figure 2 presents a few examples from Data set 2 that depict some typical liquid outflow patterns, illustrating the phase that is first observed—hence, the start of the tap—and how the tap durations may vary. The top panels of Figure 3 show the corresponding slag shares calculated by Equation (2) for the same four taps. The lower panels of the figure show, using solid squares, the corresponding 10-point normalized curves. As seen from the four examples, the evolution of the share of slag in the outflowing liquid mixture may show quite different characteristics.
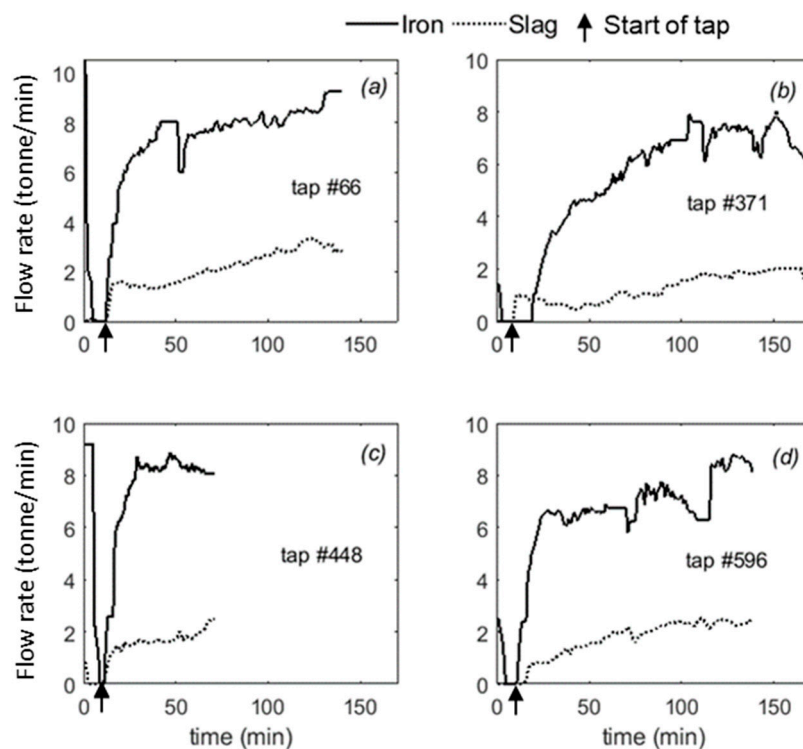
Figure 2. Examples of liquid outflow patterns from the Data set 2: (**a**) zero slag delay and 135 min tap duration, (**b**) negative slag delay and 170 min tap duration, (**c**) zero slag delay and 70 min tap duration, and (**d**) positive slag delay and 140 min tap duration.
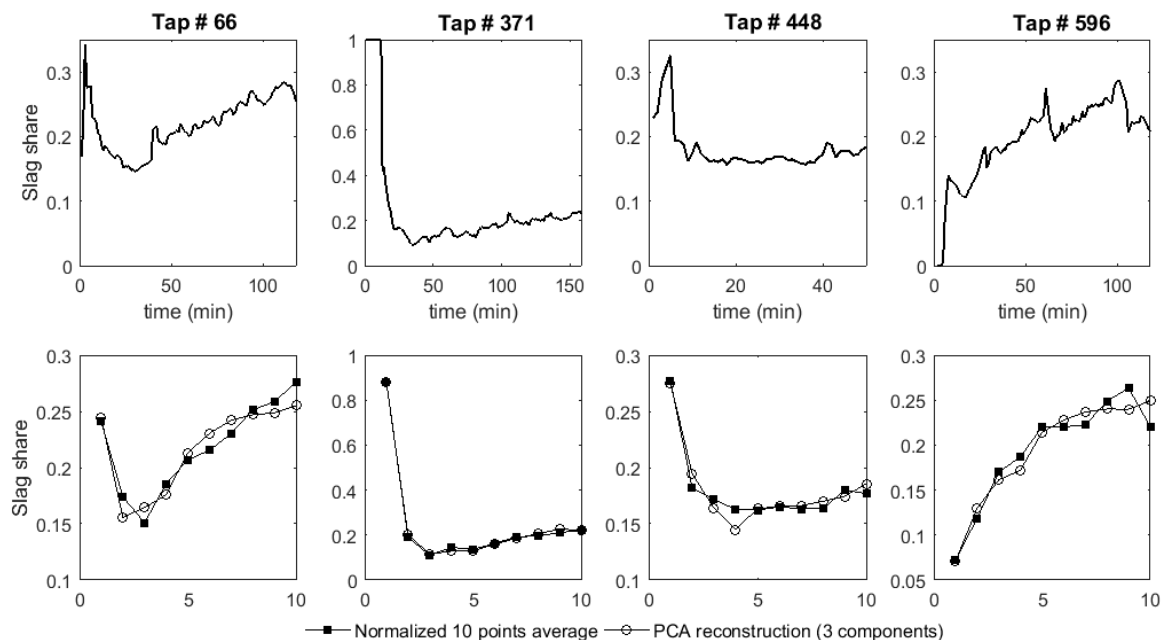

Figure 3. Slag share for the taps presented in Figure 2. Upper panels: one-minute values obtained from the measurements. Lower panels: information discretized into 10 points (solid squares) and principal component analysis (PCA) reconstruction (open circles).

A preliminary study of the normalized outflow patterns showed differences between data sets and tapholes. Figure 4 shows the slag share for the 10 average points or variables of the data sets after preprocessing. Data set 1 is presented in Figure 4a, while Data set 2 is presented for comparison

in two equivalent consecutive subsets of 720 and 763 taps in Figure 4b,c, respectively. The median curves for each taphole are depicted, as well as the median for the whole data set or subset and their corresponding 25th and 75th percentiles. The median for TH-1 in Data set 1 is seen to be similar to the 25th percentile of this dataset, while for TH-2, it is similar to the 75th percentile, particularly for variables 1 and 8–10. The median of TH-3 is, on the other hand, comparable to the global median. The median for the first subset of Data set 2 shows higher slag shares for all variables compared with Data Set 1, particularly for variable 1, where the median of TH-1 falls below the global median, while median of TH-2 falls above, and for TH-3 at the same level. Taphole median values are found above and below the global median in different orders for the other nine variables. In the second subset of Data set 2 (cf. Figure 4c), variable 1 shows a decrease from 0.35 to 0.23, with TH-1 and TH-2 medians below the global median and TH-3 above. Similar median curves are observed for variables 2–10 as in the first subset in Figure 4b.
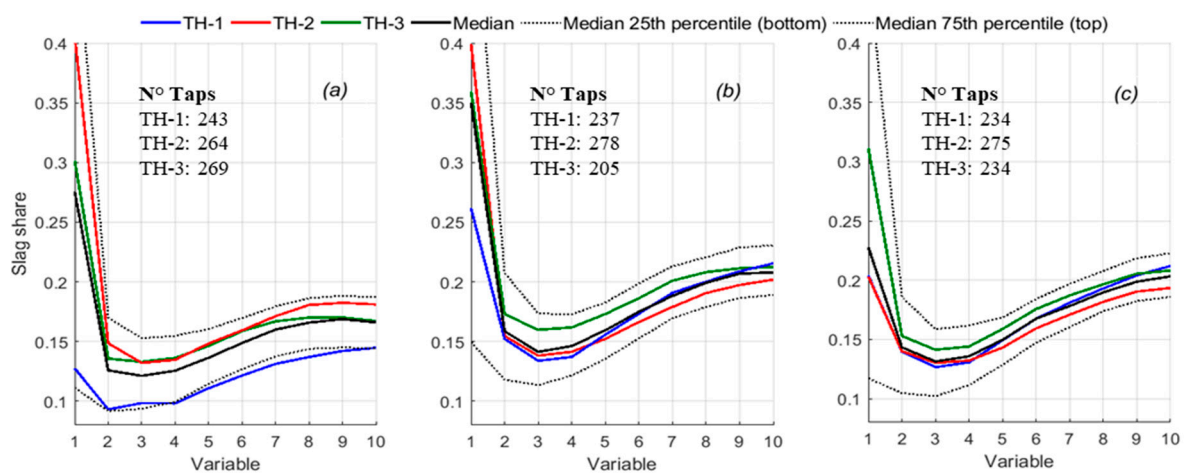

Figure 4. Overall median curves of Data set 1 and 2 and median by taphole (TH), (**a**) Data set 1, (**b**) first half of Data set 2, (**c**) second half of Data set 2.

In summary, interesting variability is observed within and between the data sets, and between the different tapholes. This motivates the effort to identify the outflow patterns that may occur during certain periods and how they persist or develop during the operation of the blast furnace. Next, a systematic PCA-based analysis of the outflow patterns of the two data sets is presented.

3.2. Post-Processing of the Results

Matlab's PCA algorithm was applied separately to the two discretized data sets. After subtracting the mean value corresponding to each variable, the algorithm computes by singular value decomposition the coefficient matrix corresponding to each variable per component. The 10-dimensional vector is represented by 10 components yielding a 10×10 coefficient matrix. The algorithm also computes the scores matrix corresponding to each observation per component, that is, there are as many individual score vectors as samples. On the basis of Equation (1) and adding the mean value of each variable, the observations can be reproduced. In this way, the variability of each component or dimension can be studied. Figure 5 presents the different pattern ranges that the first four principal components represent in the two data sets.
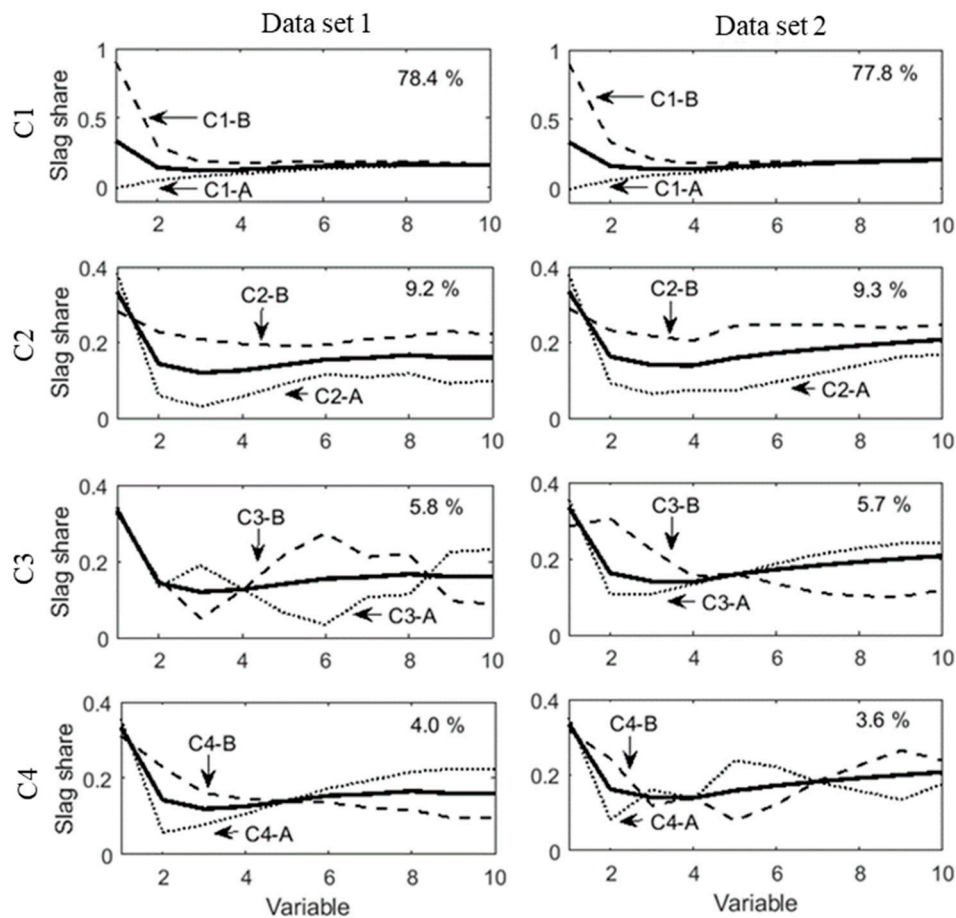
Figure 5. Slag share ranges represented by the principal component (C1 … C4) for Data set 1 (left panels) and Data set 2 (right panels). Solid lines represent the *mean pattern*, dotted lines the lowest values (labelled A), and dashed lines the highest (labelled B). The percentage of variance explained by each component is reported in the right top part of each subpanel.

After studying the results, it can be hypothesized that the first component (C1, top panels) largely reflects the slag delay expressed in terms of slag share in the initial part of the tapping, where zero corresponds to iron-first and one to slag-first drainage. The second component (C2) captures mainly the level of the slag share (excluding variable 1), falling in the range of 0.1 to 0.3 for both data sets (corresponding to a slag ratio of 110–430 kg/t_{hm}, where subscript hm denotes hot metal). The third and fourth components (C3 and C4) represent changes in the share of slag during tapping. Even though the data sets were treated separately, C1 and C2 display a similar meaningful representation of the data in the principal component space. C4 in Data set 1 and C3 in Data set 2 show similar pattern ranges as well. As seen in Figure 4, the outflow patterns of the three tapholes display different trends from variable 2 to 10, and this trend can be captured by the slopes that C4 in Data set 1 and C3 in Data set 2 describe. It can be concluded that these slopes reflect how the slag share develops during the tapping when both phases flow out. Figure 5 also indicates by solid lines the pattern corresponding to the mean values for each data set, which are seen to be very similar. In the principal component space, this pattern corresponds to the interception of the components, which is referred to as the *mean pattern* in what follows. The dotted lines correspond to lowest values in the principal component space (denoted by A) and the dashed lines correspond to highest values (denoted by B).

The algorithm also reports the percentage of the total variance explained by each component. In Data set 1, the first four components explain 78.4%, 9.2%, 5.8%, and 4.0%, respectively, while in Data set 2, they explain 77.8%, 9.3%, 5.7%, and 3.6%, respectively. Considering the meaningful information that the components provide, C1, C2, and C4 were selected for Data set 1, which together explain 91.6%

of the data variation. To provide an equal representation of the data sets and to allow for a comparison, C1, C2, and C3 were selected for Data set 2, together explaining 92.8% of the variation. An accuracy exceeding 90% was considered sufficient to represent the data sets and consequently enough to make a meaningful analysis of the results.

4. Results

The method as a batch algorithm organizes all samples in the component dimensions regardless of the taphole operated. In order to process the results, moving averages of the selected principal components for the latest 20 taps (corresponding to approximately two days of operation) were considered. The average was calculated for each taphole, taking into account the taps that occurred within the latest 20-tap window. Thus, this post-processing criterion yields a quasi-time evolution. It is important to stress that the main objective of the work is to reveal similar or different behavior of the drainage from the different tapholes to gain understanding of the variability seen during operation. The left panel of Figure 6 shows a lay-out of the three tapholes in the furnace. The right top and bottom panels present the periods during which the tapholes were operated in Data set 1 and Data set 2, respectively. Each taphole is typically operated about three weeks for the blast furnace in question. This schedule results in the alternating operation of two tapholes at the time, with some overlap (where all three tapholes are used) during the transition periods. The figure also indicates the (numbered) periods that are analyzed in the following subsections.
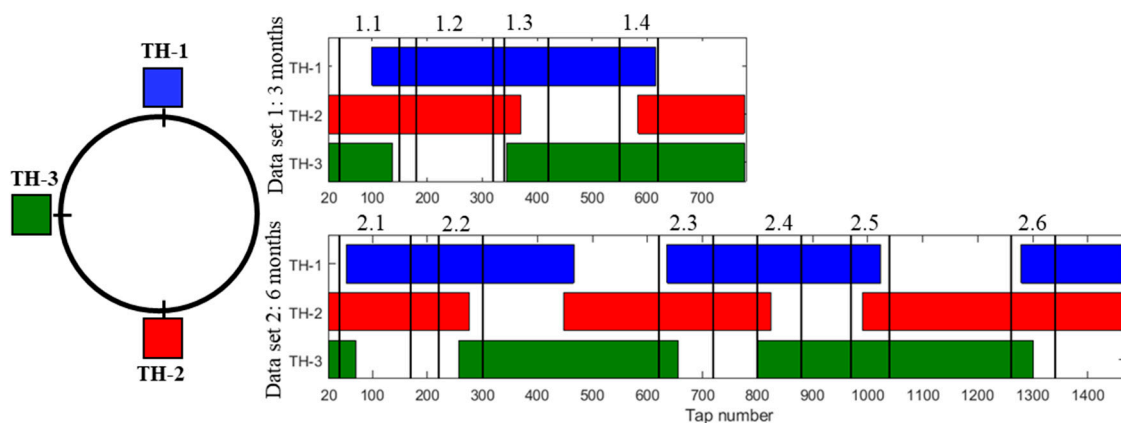

Figure 6. Taphole location in the reference furnace (**left**) and operating periods of the tapholes for the Data set 1 (**right top**) and Data set 2 (**right bottom**). The sub-periods studied in following sections are also indicated.

It should be noted that the representation, because of the data compression and averaging, does not provide detailed information about single days of operation. However, the comparison between tapholes at any given point could indicate agreement or disagreement between the outflow patterns. We will present some snapshots (cf. Figures 7–10) of the motion of the averages of the principal components as time evolves. The corresponding components of the tapholes are depicted by blue line and diamonds (TH-1), red line and squares (TH-2), and green line and circles (TH-3). For the sake of clarity, the two most important components (C1 and C2) are plotted versus each other in a "phase plot" for shorter sub-periods (cf. Figures 7 and 9).

The positions of the markers on each curve indicate the average value of the components corresponding to each tapholes for the last 20 observations. For instance, a blue diamond labeled "70" indicates the average location in the principal component space of taps from TH-1 from taps 50 to 70 regardless of taphole. As the tapholes are operated alternatively, the same number label will appear next to the markers on the curves of the operating tapholes, indicating the pattern progression. For clarity, arrows show the direction of the evolution, and labels "start" and "end" are used to

indicate the first and last points of operation of a taphole if it occurs in the period. On the axes of each component, the limits of the component (lower by A, upper by B, cf. Figure 5) are also indicated. In addition to the phase plot of C1 and C2, similar averages of an additional principal component, C4 for Data set 1 (cf. Figure 8) and C3 for Data set 2 (cf. Figure 10), are plotted in a separate panel for each data set along with the average tap duration of the operating tapholes.

4.1. Data Set 1

Figure 7 presents C1 versus C2 for Data set 1, while Figure 8 depicts the evolution of C4 and the tap duration. Four periods are studied from Data set 1, referred to as Periods 1.1–1.4 (cf. Figure 6). They range from 7 to 16 days of operations and include segments of operation where one taphole is replaced by another, as well as segments where a taphole pair operates.

4.1.1. Period 1.1

Figure 7a shows the evolution of C1 versus C2 for Period 1.1 ranging from tap 40 to 150 and corresponding to 15 days of operation. Initially, TH-2 and TH-3 operate with stable outflow patterns with little variation for taps 40–70. TH-2 shows short negative slag delay (positive C1) where slag flows out first, while TH-3 shows a short positive slag delay (negative C1) where iron flows out first. This slight imbalance can be explained by the reasoning presented in Figure 1. By tap 70, both tapholes exhibit outflow patterns resembling the mean. However, at the time when TH-1 starts operating (after tap 100), TH-3 has shifted towards a higher slag share (positive C2). As TH-1 initially drains a relatively high share of iron, the system reacts to compensate for such an imbalance with TH-3. The balance before this moment and the imbalance that follows are also seen in C4 in the top panel of Figure 8. By tap 130, the drainage reaches a more stable distribution, with TH-1 showing a positive slag delay and TH-2 and TH-3 a negative slag delay. After TH-3 ends its operation, TH-1 and TH-2 show little variation, with TH-1 draining more iron than TH-2. One-day stoppages occur at taps 74 and 141, but do not affect the drainage patterns.

Figure 8, in turn, shows that C4 values higher than the mean occur when the tap duration is short. As seen in Figure 5, high C4 values correspond to a negative slope of slag share. Thus, if the slag share is high at the beginning of the tapping and, as a consequence, the descent of the slag–gas interface is rapid, a short tap duration can be expected because the moment when the slag–gas interface bends down to the taphole will end the tap [9] (cf. Figure 1). This holds true for TH-1 and TH-2 beyond Period 1.1.

4.1.2. Period 1.2

Figure 7b shows C1 versus C2 for taps 180–320, corresponding to the 16 days of operation in Period 1.2 that starts two days after the end of Period 1.1. Period 1.2, where TH-1 and TH-2 operate alternately, is particularly interesting because the tapholes are opposite (cf. Figure 6), so possible differences in the in-hearth conditions should be discerned during the period. The results indeed suggest drainage imbalance: at tap 180, TH-1 and TH-2 display similar patterns to those seen at the end of Period 1.1, that is, positive slag delay for TH-1 and negative for TH-2. For taps 180–210, the slag share decreases in TH-1, while it increases in TH-2 and the outflow patterns remain fundamentally different, but from tap 210 onward, the imbalance gradually disappears and the patterns become more similar. By tap 255, the two tapholes show patterns where the two liquids flow out simultaneously. TH-2 still drains a higher share of iron than TH-1, but the differences gradually become smaller, even though TH-1 still drains iron first while TH-2 drains slag first. As for C4, in Period 1.2 (like the previous period), a negative correlation is seen with the tap duration (cf. Figure 8). The taphole showing a larger C4 value changes from one to the other, in pace with the taphole showing the shortest tap duration. In the end of this period, all principal components considered approach the mean values for both tapholes, but the strong imbalance lasted for about 100 taps of operation of the taphole pair, reflecting the slow dynamics of the system.
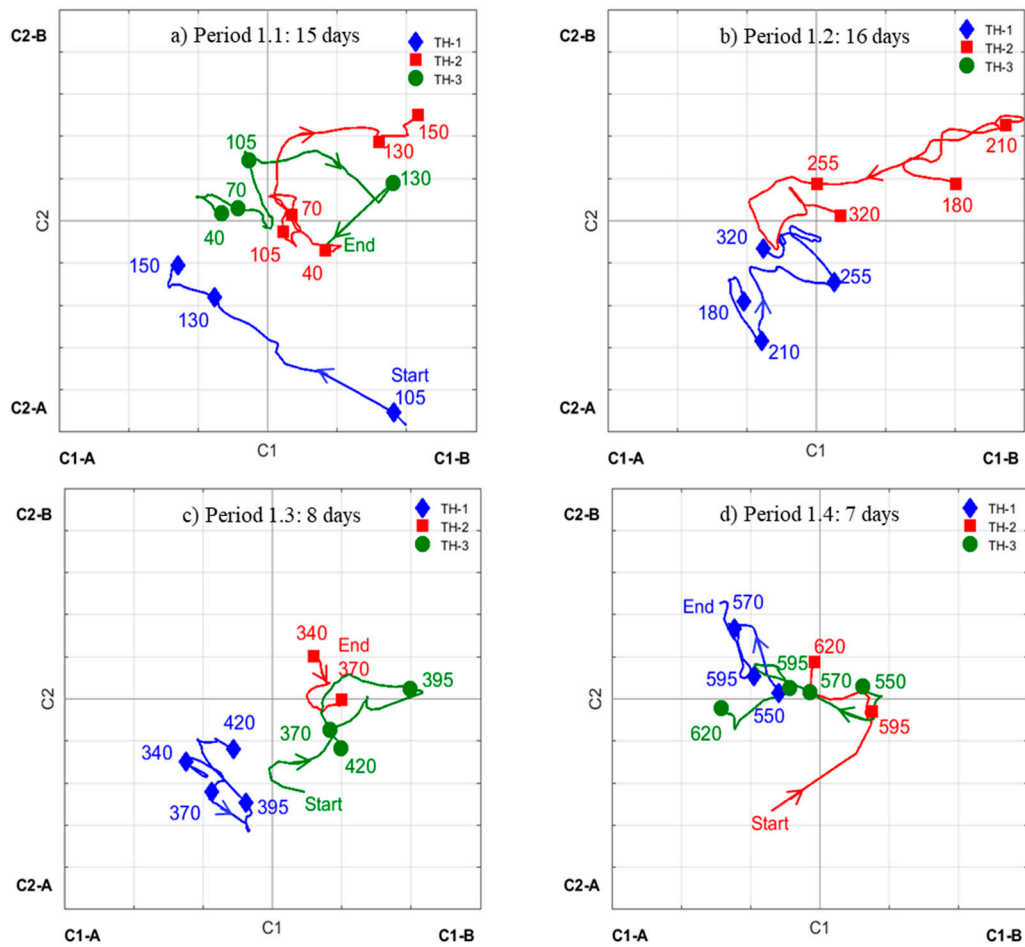
Figure 7. First vs. second principal components progression (C1, C2) corresponding to Data set 1 at different tap labels. (**a**) Period 1.1, (**b**) Period 1.2, (**c**) Period 1.3, (**d**) Period 1.4.
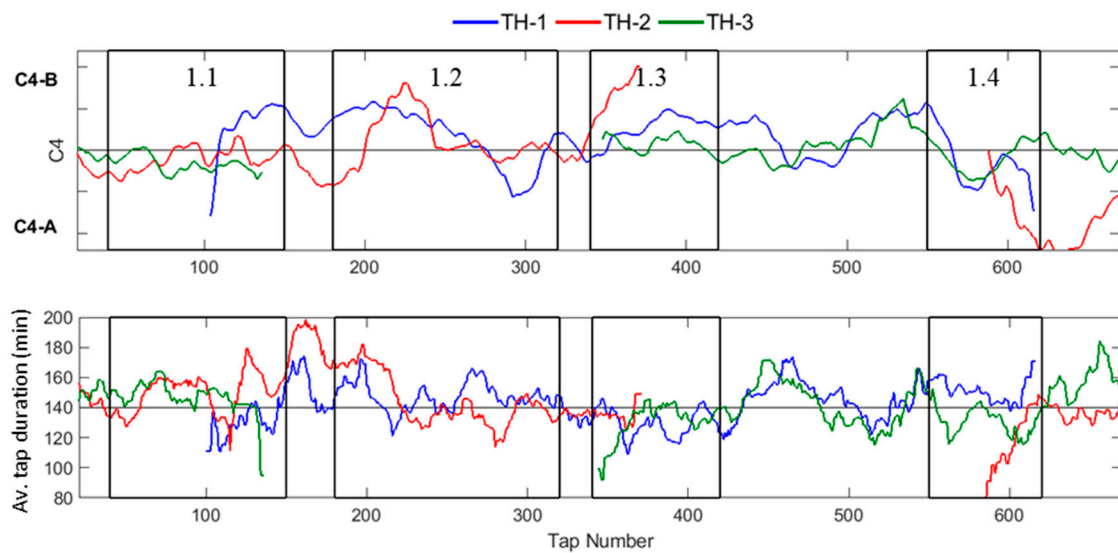

Figure 8. Fourth principal component (C4, **top**) and average tap duration (**bottom**) corresponding to the four periods of Data set 1. Blue line (TH-1), red line (TH-2), and green line (TH-3).

4.1.3. Period 1.3

Figure 7c shows the period between taps 340 and 420, starting two days after Period 1.2 ended. It covers eight days of operation, where TH-2 ends while TH-3 starts its operation. At tap 340, TH-1 and TH-2 show outflow patterns of similar characteristics to those in the previous period: TH-1 with lower slag share and iron-first flow and TH-2 with higher slag share and slag-first flow. In this drainage state, the "incoming" taphole TH-3 starts with a simultaneous drainage of both liquid phases and with a slightly higher iron share than what TH-1 exhibited initially in Period 1.1. This suggests that at the moment when TH-3 starts its operation, the iron–slag interface is at the taphole level. For taps 370–395, TH-3 adopts the same performance that TH-2 showed before its operation ended. However, by tap 420, both TH-1 and TH-3 drain a higher iron share, but a positive and negative slag delay, respectively. This drainage state should trigger an imbalance in the systems as more iron is drained than produced, but may reflect a temporal state (with low slag rate). Yet, the internal conditions still seem to allow for a rather uniform liquid flow within the hearth. Figure 8 shows that all three tapholes yield medium or high C4 values and short or average tap durations.

4.1.4. Period 1.4

The results of the final period of Data set 1, starting six days after Period 1.3 has ended and lasting for seven days ranging from tap 550 to 620, are shown in Figure 7d. At tap 550, both TH-2 and TH-3 show a slag share close to the average (0.2) and short positive and negative slag delays, respectively. As expected, the slag share increased after Period 1.3, and the increase continues in TH-1. TH-3 shows little variation in the share of slag, but shifts to a positive slag delay around tap 595. By contrast, the slag share for TH-2, which is taken into operation, increases rapidly. The tap duration for TH-1 is considerable longer than for TH-3 (cf. Figure 8), suggesting that the system reaches a balanced drainage state mainly through changes in the outflows of TH-1.

4.2. Data Set 2

Figure 9 presents the C1 versus C2 for Data set 2 and Figure 10 the results for C3 in the top panel and tap duration in the bottom panel. Six periods are studied (cf. Figure 6), with period lengths ranging from 9 to 16 days of operation, including segments where one taphole starts its operation and another ends it.

4.2.1. Period 2.1

Figure 9a shows the evolution of C1 versus C2 for Period 2.1, taps 40–170, corresponding to 16 days of operation of Data set 2. TH-1 starts operating around tap 50 with a long positive slag delay, but with a higher drained share of slag compared with the other tapholes. Figure 10 confirms these features by showing a low C3 value, that is, a positive slope of the slag share: as iron drains first, the slag outflow rate is small initially, but increases as the iron level descends and the taphole erodes. As expected, the tap duration is long; an initial high iron share indicates a high iron level in the hearth and a longer time will elapse until the slag–gas interface has descended sufficiently to end the tapping. However, as the operation continues, the slag share steadily decreases in TH-1. Inspection of the individual outflows from this taphole during the period revealed that the iron flow of some taps was interrupted or highly irregular. This suggests an unsuccessful drainage of iron from the taphole, even though iron was initially the first phase to flow out. For TH-3, the outflow patterns fall close to the mean and vary little during the last 30 taps of this taphole. As for TH-2—taphole that operates throughout the whole period—fluctuations between positive and negative slag delays are observed, but with low variation in C2 and an overall slag share close to 0.2. With time, both TH-1 and TH-2 converge around tap 170 to similar patterns with short negative slag delays. The tap duration decreases for both tapholes, which may indicate a poor slag drainage. C3 in Figure 10 also indicates

that from tap 170 onwards, TH-1 shows a negative slope, that is, the iron share increases as the tapping progresses. This is a significant pattern shift from the drainage in the earlier parts of the period.
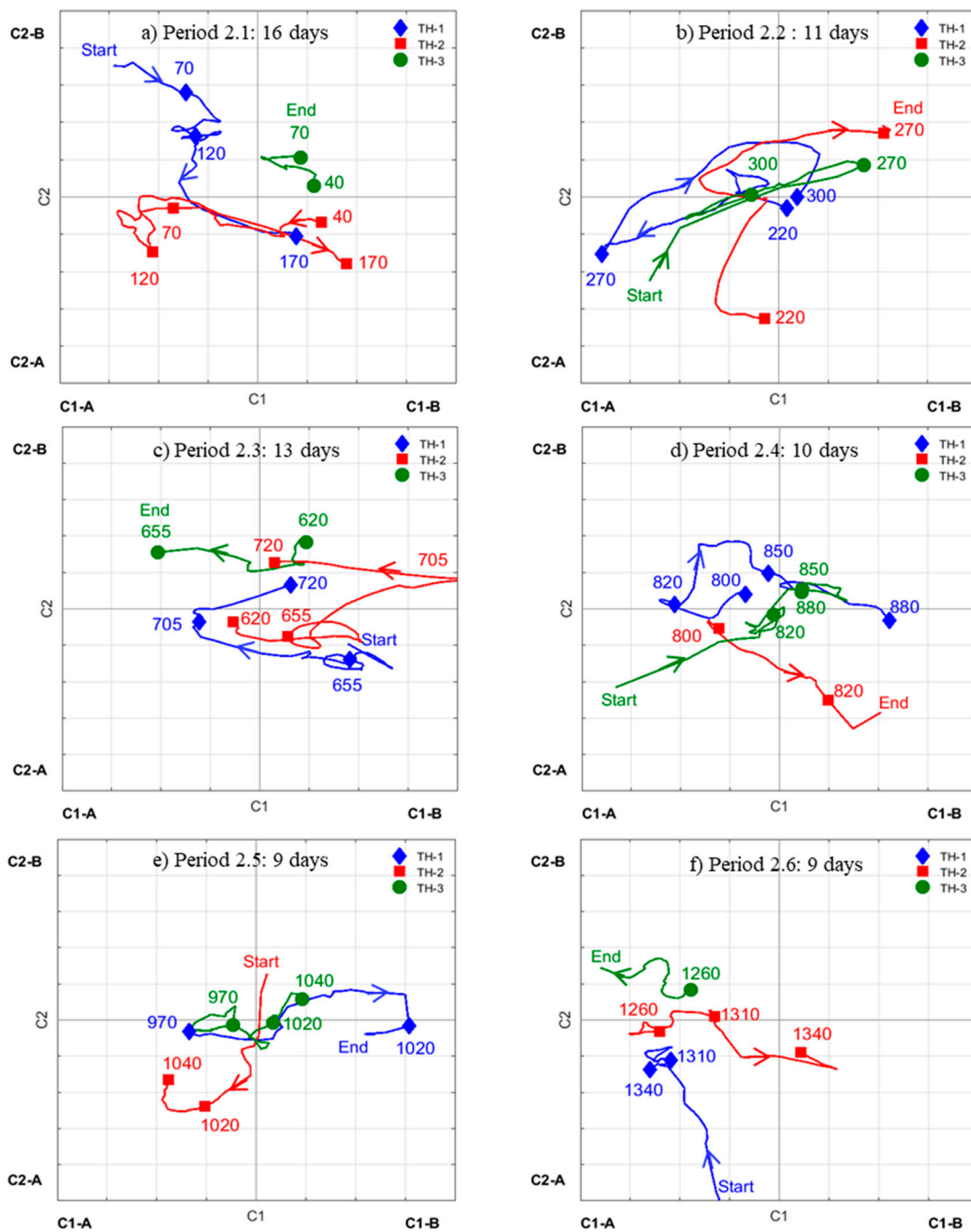

Figure 9. First vs. second principal components progression (C1, C2) corresponding to Data set 2 at different tap labels. (**a**) Period 2.1, (**b**) Period (2.2), (**c**) Period 2.3, (**d**) Period 2.4, (**e**) Period 2.5, (**f**) Period 2.6.
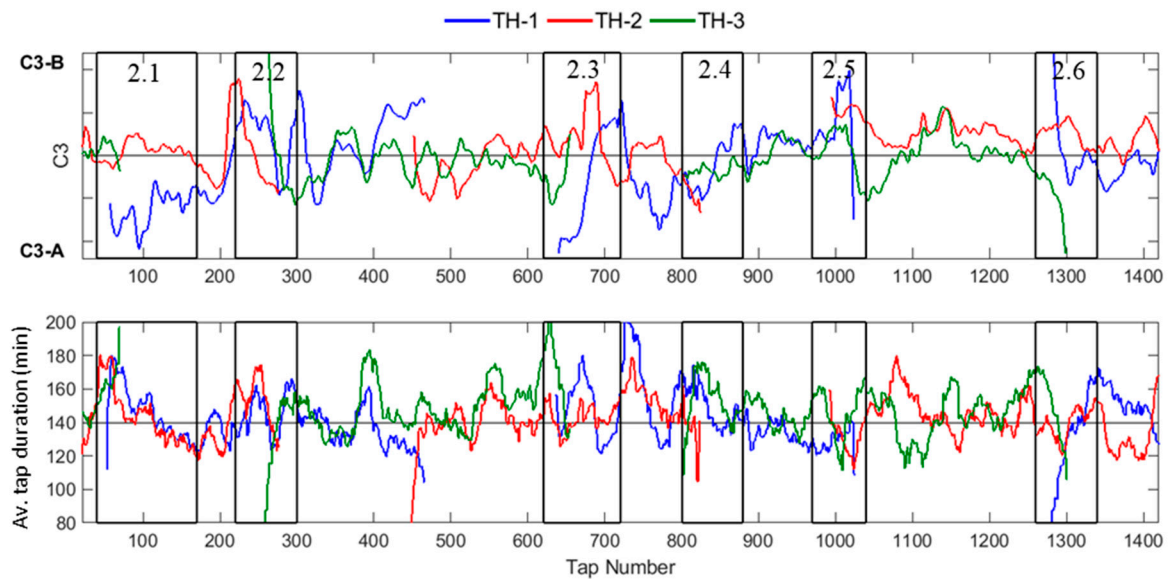
Figure 10. Third principal component (C3, **top**) and average tap duration (**bottom**) corresponding to the six periods of Data set 2. Blue line (TH-1), red line (TH-2), and green line (TH-3).

4.2.2. Period 2.2

Period 2.2 (Figure 9b), with taps 220–300, covering 11 days of operation, shows another type of evolution of the principal components. TH-1 operates throughout the period, TH-2 up to tap 270, while TH-3 is taken into operation some taps earlier. TH-1 shows a cyclical evolution in the (C1, C2) plane, where C1 first decreases and then increases back to the level of the starting point, while the changes in C2 are smaller. Thus, the main differences are in the slag delay, which changes from zero to clearly positive, and then back again. By contrast, for TH-2, taps 220–270, which represent the last 50 taps with this taphole operating, the main change is seen in C2: the operation shifts from a low slag share towards a high one with no slag delay, finally drifting to a state with a negative slag delay. A descent of the iron–slag interface in the hearth at TH-2 could lead to an increase of the slag share in the tapping and eventually also to a negative slag delay. By tap 270, TH-1 drains enough iron to lower the iron–slag interface to yield a negative slag delay (cf. Figure 1b) for TH-2, as it is ending its operation, and for TH-3, a few taps after its operation starts. Such behavior is discussed at some length in the work of [17]. C3 for TH-2 (Figure 10), in turn, indicates that the slope of the slag share increases, which can also be explained by the descent of the iron–slag interface. As TH-3 is taken into operation, the taps initially show a low slag share, but the outflow patterns rapidly change to become similar to those of TH-2 (around tap 270). Compared with Period 2.1, the tap duration for TH-1 is shorter as C2 decreases and C3 increases, even though C1 stays low.

Summarizing the findings, the changes in the hearth during the period reflect a strong imbalance in the liquid volumes tapped from the tapholes. Measures in the casthouse taken at the beginning and at the end of the period, for example, different tapping sequences or the use of different drill diameters, may trigger such an imbalance. Nonetheless, local conditions in certain hearth regions or taphole conditions cannot be ruled out as influencing factors. More information about specific taps should be analyzed in order to explain the reason for the imbalance observed.

In the six-week segment between Periods 2.2 and 2.3 (not shown), TH-1 shows some variation of the slag delay, but the overall slag share stays close to the mean. TH-3 initially shows a negative slag delay and then drifts towards the mean pattern, and to a positive slag delay as TH-2 is taken into operation. This "new" taphole starts its operation with a long positive slag delay and high iron share to converge to the states of the other two tapholes, suggesting that liquid levels are in balance in the different regions of the hearth. The changes in slopes described by C3 in the top panel of Figure 10 may

reflect the system's response to maintain such a balance. Like in previous periods, a positive slope (lower C3) implies longer tap duration. For taps 500–620, the outflows from TH-2 and TH-3 show less variation in the three principal components, despite a six-day stoppage after tap 603.

4.2.3. Period 2.3

Figure 9c presents the evolution of (C1, C2) for the period that spans from taps 620 to 720, corresponding to 13 days of operation. This period occurs after a six-day stoppage, where operation restarts with tap 604. Thus, tap 620 in the (C1, C2) plane represents the average location of the 16 taps after operation was resumed. TH-3 ends its operation as TH-1 is taken into use. At tap 620, the principal components for TH-2 suggest drainage close to the mean pattern, while the flow from TH-3 has a higher slag share. Thus, it is expected that TH-1, when introduced (replacing TH-3), will count with a higher iron share, as is also seen in C2. TH-1 initially shows a high iron share and negative slag delay, to later show higher a slag share. Also, the slag delay changes from negative to positive and then negative again. The behavior of TH-2 is almost opposite, indicating that the end levels of the iron–slag interface show a mirror relation (noting that TH-1 and TH-2 are opposite tapholes). Finally, the outflows of TH-1 and TH-2 converge to similar patterns by tap 720. C3 indicates a progressive change in opposite directions of TH-1 and TH-2 before tap 700 to then reach a more balance distribution around the mean. A negative correlation between C3 and tap duration is again observed.

4.2.4. Period 2.4

Period 2.4 represents seven days of quite stable and uniform operation (Figure 9d, taps 800–880), where TH-1 operates throughout the period, TH-2 ends, and TH-3 starts its operation in the beginning of the period. TH-1 and TH-2 initially display a slightly positive slag delay and a mean slag share of 0.2, and as TH-3 is introduced, a positive slag delay is also expected. However, local conditions or operating actions result in a high iron share for TH-3, inducing imbalance as explained in Figure 1. At tap 820, TH-3 drains according to the mean pattern without slag delay, and the high iron share of TH-2 is counteracted by a shift in outflow of TH-1 to a higher slag share. The variations in C3 for all tapholes are small (Figure 10). After TH-2 is taken out of operation, the other tapholes show stable outflows, but TH-1 drifts towards a state with negative slag delay.

4.2.5. Periods 2.5 and 2.6

Period 2.5 (Figure 2e) represents a nine-day segment (taps 970–1040) that holds both positive and negative slag delays, but the slag share varies little. It can be argued that similar drainage conditions prevail at the tapholes with a uniform distribution of the liquids in the hearth. However, at the point where TH-1 is substituted by TH-2 (before tap 1020), its iron drainage has become poor: TH-1 experiences problematic taps much more often than TH-2 and TH-3. As a result, TH-2 drifts to a higher iron share and positive slag delay by tap 1020. Even though TH-2 drains enough iron, the tap duration is short, suggesting that slag is also poorly drained. As a consequence, both TH-2 and TH-3 show a higher slag share in the outflows by tap 1040. The imbalance of the drainage system is also seen in C3, but for taps 1050–1250, a more stable operation is noticed. This can be compared to similar segments following periods with a larger variation, for example, taps 350–600 and taps 800–100.

Finally, Period 2.6 is studied, which represents the nine-day segment with taps 1260–1340. During this period, TH-1 starts operating, while TH-3 ends. As also seen in Period 2.4, when both operating tapholes show iron-first tapping (i.e., positive slag delay), the "incoming" taphole will also do so. The initial imbalance in the share of slag drained between TH-1 and TH-2 vanishes by tap 1310, when TH-3 has already been taken out of operation. TH-1 maintains a long positive slag delay until tap 1340, while TH-2 shifts to a negative one, but towards the end of Data set 2, the outflows of the two tapholes fall close to the mean.

5. Results of PCA and Liquid Level Model

The large hearth diameter in multi-taphole blast furnaces may give rise to zones of different coke-bed permeability, which leads to differences in the local conditions and liquid levels [18,19]. A mathematical model was developed by the present authors [14] and applied to study the effect of different parameters and variables on the liquid levels and drainage process. The hearth was modelled as two interconnected pools of liquids, where communication factors can control the flow from one taphole zone to the other. Figure 1 illustrates the states of a hearth with good communication between the zones, resulting in uniform liquid levels (except the in/declining parts in the vicinity of the tapholes). A sensitivity analysis of the model was conducted to evaluate the effect of parameters on the tap duration and slag delay. Therefore, some findings from the earlier study can be associated with the PCA results presented here.

For instance, the model shows that poor iron communication increases the tap duration and slag delay (Periods 2.1, 2.3, and 2.4), while poor slag communication does not change the tap duration, but results in a negative slag delay (Periods 1.3 and 2.3). Asymmetric cases, where the pool sizes are different, give rise to conditions resembling those observed during periods when one taphole ends its operation and another is taken into use. Roche et al. [14] demonstrated that the asymmetric cases are characterized by more negative slag delay (for one taphole) and longer tap duration (for the other). This is observed in periods where the "incoming" taphole shifts from an initially positive slag delay to a slight negative one after some taps (Periods 1.3, 2.1, 2.2, and 2.4).

Changes in the conditions in front of the taphole due to the interaction between the injected mud and the coke bed [5] could potentially alter the internal level of the taphole with respect to the slag–iron interface, causing differences in the slag delay and tap duration between operating tapholes. The final declivity of the gas–slag interface is affected by the slag viscosity and coke diameter [20–22], which may vary with time and affect the tap duration, and, therefore, the liquid levels, triggering some imbalance.

Regardless of the conditions in the hearth, the outflow from one taphole will affect the outflow of the other. A sensitivity study of the outflow parameters by the model suggests that the system is prompted to changes in slag delay and tap duration when different outflow patterns are imposed on one taphole. A slower initial drainage rate of iron from one taphole yields a positive slag delay and longer tap duration for the other, which, in turn, leads to a negative slag delay for the first taphole because of low liquids levels (cf. Figure 1). This behavior is seen in several periods where the outflow patterns are found in opposite regions of the (C1, C2) plane (Periods 1.1, 1.2, 1.3, 2.4, and 2.6). On the other hand, a slow initial drainage rate of slag from one taphole yields slightly negative slag delays in both tapholes and longer tapping. This seems to be the case with tapholes ending their operation when compared with the operating one (Periods 1.3, 2.1, and 2.5). As observed in the results, the outflow patterns diverge as a result of a triggering factor, but often converge after some period of operation towards the mean pattern as the systems reaches balance again (as seen in Periods 1.2, 1.4, 2.2, and 2.4). A constant monitoring of the variables during operation, for example, iron production, liquid outflows, and slag delay, is a key to keep such imbalances within reasonable limits.

6. Summary of the Analysis

For the taps in the two data sets analyzed, TH-1 entered into operation four times, while TH-2 and TH-3 entered three times. Even though the data sets analyzed were quite extensive, the number of taphole changes was still limited, and it is thus difficult to draw general conclusions about the draining conditions of the taphole that is brought into operation. However, it can still be deduced that if the taphole that enters into operation is located farther off (here, TH-1 or TH-2) and the liquids are not in balance, it likely leads to more imbalance in the drainage. This is particular notable for TH-1 in Periods 1.1, 2.1, and 2.6. This effect can be caused by smaller random effects, for example, in the conditions in the coke bed at the taphole inlet that accentuate the characteristics of the pattern when a taphole starts operating. Thus, an existing drainage imbalance sets the incoming taphole in an extreme initial state. On the other hand, when the drainage of the system is balanced, the operation

of the incoming taphole is not very different, even though it often initially shows some discrepancy in terms of (typically positive) slag delay and slag share. This suggests that inactivity of a taphole gradually leads to different conditions in the hearth in the vicinity of it. In the reference BF, the taphole length was found to be initially considerably longer for the fresh taphole compared with the ones that had been operating. As for the end of the operating period of a taphole pair, more extreme drainage patterns were often observed. In the steel works in question, the incoming and outgoing tapholes were operated alternately for a few taps, most likely to induce a smooth transition, but disturbances were still seen. This also supports the hypothesis that different local conditions in the hearth may arise, such as different liquid levels and differences in the hearth-coke permeability. The model-based analysis of the liquid levels referred to in Section 5 indicated that the effective pool of the hearth that is drained may grow during tapping [14]. Such distribution of volumes would not only lead to different outflow patterns, but could also induce zones with different permeability with impact on lining and taphole erosion.

Also, the results of C4 for Data set 1 and C3 for Data set 2 are interesting because of the cyclical trend seen for all tapholes. These principal components showed negative correlation with the tap duration in both data sets and for all three tapholes. As mentioned earlier, with an initial higher slag share in the outflow, the slag–gas interface descends more rapidly. Additionally, some variation of the slag share as the tapping evolves is expected as a result of taphole erosion. Another explanation is that the fluid dynamics of the system induces such behavior, for example, the fact that iron has to be elevated from levels below the taphole.

It should be stressed that the two-phase outflow, the unknown conditions of the coke bed and the taphole entrance, and the taphole erosion make it difficult to explain the dynamics of the system. In general, TH-3 showed a more uniform distribution of the samples around the mean pattern, most likely owing to its location in the hearth. When operating alternately with either of the other two tapholes, similar hearth conditions are expected because of their location. Further, TH-1 and TH-2 often showed opposite behavior in order to balance the drainage.

The liquid level model supporting the findings [14] has proposed some system parameters that affect the outflow patterns of iron and slag. In light of the information gained in the present study, there may be a need to re-evaluate the system with the model. A challenge is that every tapping seems to show individual features, but the results presented in this paper still reveal some general drainage patterns of the hearth, and interrelations between the drainage of two alternating tapholes. In particular, it would be interesting to understand the transition paths between different common or particular outflow patterns, which could be useful when an online model is developed. In order to present more conclusive interpretations, a larger number of samples is necessary, where each taphole is represented by a sufficient number of operating periods. Despite these limitations, the PCA-based tool must be considered efficient in illustrating and condensing the information from individual samples into a comprehensible and compact form. The tool can be used along with other information from the BF to analyze how the system reacts after stoppages of different duration, an increase or decrease in the production rate, interchanges of tapholes, changes of drill diameters, and other specific measures taken in the casthouse.

7. Conclusions

Two data sets, corresponding to three and six months of operation of a blast furnace, were analyzed with respect to the drainage of the furnace hearth. The blast furnace studied has three tapholes (TH-1, TH-2, and TH-3) and the liquid outflow rates were calculated based on weighing of the torpedos (hot metal) and signals from the granulation unit (slag). After inspecting individual outflow rates throughout the data, certain outflow patterns were detected and some of them were found to recur. To simplify the interpretation, the share of slag in the outflow was taken as the variable of primary concern. After normalizing the tap duration, the evolution of the share of slag during the tapping was down-sampled to ten variables to filter out some noise. To further compress the information

and to make it possible to visualize the time evolution of the drainage patterns, principal component analysis (PCA) was applied to the data sets. The results of the compression were analyzed and the first two principal components were found to describe two relevant tapping features: the first principal component (C1) basically describes the slag delay (i.e., the length of the period of one-phase flow in the beginning of the tapping), and the second principal component (C2) describes the mean or end slag share for the tapping. To better analyze the results, one additional component was considered, which expresses how the slag share develops as both iron and slag are being drained. This component was found to be the fourth component (C4) in Data set 1 and the third component (C3) in Data set 2. For the sake of clarity, the results were post-processed into moving averages over the latest 20 taps. The results presented in the paper focus mainly on detecting diverging or converging behavior of the outflows of the operating tapholes based on the evolution of the principal components. The data sets were divided into different periods. TH-1 was found to display the most erratic patterns, followed by TH-2, while TH-3 exhibited less fluctuation. This is logical, as TH-3 is located between TH-1 and TH-2. Often, taphole changes were followed by draining imbalance, where the outflows from all three tapholes occasionally showed large fluctuations, which were seen as extreme values in the principal component space. After some time, the system typically stabilized, leading to drainage that corresponded to the mean outflow pattern. Even though the reason for the disturbances often remained unknown, the general behavior of the system could partly be explained by arguments based on fluid dynamics. To generalize the findings, a longer data set may be needed, because random events seem to have a considerable effect on the dynamics. Nonetheless, the PCA-based tool developed has proven to be useful in capturing the evolution of hearth drainage in a few key indices, which may be studied and analyzed in an attempt to gain further understanding of the complex industrial system at hand. To assess the usefulness of the PCA-based approach, it is proposed that the model should be implemented in the plant and the evolution of the (main) principal components could be studied and correlated with other BF variables. This will allow for gathering further experience on what affects the lower-dimensional representation of the liquids outflows and how the information could be utilized in the casthouse operation. In conjunction with further analysis, the accuracy of the estimated liquid outflow rates should also be evaluated, and, in particular, the quality of the estimated slag outflow rate.

Author Contributions: conceptualization, M.R. and H.S.; methodology, M.R.; software, M.R.; formal analysis, M.R., M.H., and H.S.; data curation, M.H.; writing—original draft preparation, M.R.; writing—review and editing, M.R., M.H., and H.S.; supervision, M.H. and H.S.; funding acquisition, H.S.

Conflicts of Interest: The authors declare no conflict of interest.

References

1. Iida, M.; Ogura, K.; Hakone, T. Numerical Study on Metal/Slag Drainage Rate Deviation during Blast Furnace Tapping. *ISIJ Int.* **2009**, *49*, 1123–1132. [CrossRef]
2. Iida, M.; Ogura, K.; Hakone, T. Analysis of Drainage Rate Variation of Molten Iron and Slag from Blast Furnace during Tapping. *ISIJ Int.* **2008**, *48*, 412–419. [CrossRef]
3. Nouchi, T.; Sato, M.; Takeda, K.; Ariyama, T. Effects of Operation Condition and Casting Strategy on Drainage Efficiency of the Blast Furnace Hearth. *ISIJ Int.* **2005**, *45*, 1515–1520. [CrossRef]
4. Roche, M.; Helle, M.; van der Stel, J.; Louwerse, G.; Shao, L.; Saxén, H. On-Line Estimation of Liquid Levels in the Blast Furnace Hearth. *Steel Res. Int.* **2019**, *90*, 1800420. [CrossRef]
5. Tsuchiya, N.; Fukutake, T.; Yamauchi, Y.; Matsumoto, T. In-furnace Conditions as Prerequisites for Proper Use and Design of Mud to Control Blast Furnace Taphole Length. *ISIJ Int.* **1998**, *38*, 116–125. [CrossRef]

6. Zhao, Y.; Fu, D.; Lherbier, L.W.; Chen, Y.; Zhou, C.Q.; Grindey, J.G. Investigation of Skull Formation in a Blast Furnace Hearth. *Steel Res. Int.* **2014**, *85*, 891–901. [CrossRef]

7. Takatani, K.; Inada, T.; Takata, K. Mathematical Model for Transient Erosion Process of Blast Furnace Hearth. *ISIJ Int.* **2001**, *41*, 1139–1145. [CrossRef]

8. Panjkovic, V.; Truelove, J.S.; Zulli, P. Numerical modelling of iron flow and heat transfer in blast furnace hearth. *Ironmak. Steelmak.* **2002**, *29*, 390–400. [CrossRef]

9. Tanzil, W.B.U.; Zulli, P.; Burgess, J.M.; Pinczewski, W.V. Experimental Model Study of the Physical Mechanisms Governing Blast Furnace Hearth Drainage. *Trans. Iron Steel Inst. Jpn.* **1984**, *24*, 197–205. [CrossRef]

10. Nishioka, K.; Maeda, T.; Shimizu, M. A Three-dimensional Mathematical Modelling of Drainage Behavior in Blast Furnace Hearth. *ISIJ Int.* **2005**, *45*, 669–676. [CrossRef]

11. Agrawal, A.; Kor, S.C.; Nandy, U.; Choudhary, A.R.; Tripathi, V.R. Real-time blast furnace hearth liquid level monitoring system. *Ironmak. Steelmak.* **2016**, *43*, 550–558. [CrossRef]

12. Saxén, H. Model of Draining of the Blast Furnace Hearth with an Impermeable Zone. *Metall. Mater. Trans. B* **2015**, *46*, 421–431. [CrossRef]

13. Saxén, H.; Brännbacka, J. Dynamic model of liquid levels in the blast furnace hearth. *Scand. J. Metall.* **2005**, *34*, 116–121. [CrossRef]

14. Roche, M.; Helle, M.; van der Stel, J.; Louwerse, G.; Shao, L.; Saxén, H. Off-line Model of Blast Furnace Liquid Levels. *ISIJ Int.* **2018**, *58*, 2236–2245. [CrossRef]

15. Bartholomew, D.J. Principal Components Analysis. *Int. Encycl. Educ. (Third Ed.)* **2010**, 374–377. [CrossRef]

16. Kourti, T. 4.02 Multivariate Statistical Process Control and Process Control, Using Latent Variables. *Compr. Chemom.* **2009**, 21–54. [CrossRef]

17. Helle, M.; Roche, M.; Saxén, H. On-line estimation of liquid levels and local drainage characteristics in the blast furnace. In Proceedings of the SteelSim, Toronto, ON, Canada, 13–15 August 2019. paper 24.

18. Hu, X.; Sundqvist Ökvist, L.; Ölund, M. Materials Properties and Liquid Flow in the Hearth of the Experimental Blast Furnace. *Metals* **2019**, *9*, 527. [CrossRef]

19. Nishioka, K.; Maeda, T.; Shimizu, M. Effect of Various In-furnace Conditions on Blast Furnace Hearth Drainage. *ISIJ Int.* **2005**, *45*, 1496–1505. [CrossRef]

20. Fukutake, T.; Okabe, K. Experimental Studies of Slag Flow in the Blast Furnace Hearth During Tapping Operation. *Trans. Iron Steel Inst. Jpn.* **1976**, *16*, 309–316.

21. Fukutake, T.; Okabe, K. Influences of Slag Tapping Conditions on the Amount of Residual Slag in the Blast Furnace Hearth. *Trans. Iron Steel Inst. Jpn.* **1976**, *16*, 317–323.

22. Zulli, P. Blast Furnace Hearth Drainage with and without a Coke Free Layer. Doctoral Dissertation, Faculty of Engineering, UNSW, Sydney, Australia, 1991.